Structure of a source-driven magnetized oblique presheath

Devendra Sharma* and H. Ramachandran†
Institute for Plasma Research, Bhat, Gandhinagar 382 428, Gujarat, India
(Received 11 September 2001; revised manuscript received 15 February 2002; published 26 August 2002)

A source-driven magnetized presheath is analyzed in an obliquely incident magnetic field. The conventional fluid treatments of the collisionless and collisional magnetized presheath use standard fluid equations to recover the velocity profiles that satisfy the Bohm sheath criterion at the electrostatic sheath edge. In a purely source-driven collisionless presheath, however, there is no mechanism to redistribute the change in parallel energy in the perpendicular direction and therefore the boundary values of flow velocities are strong functions of angle of incidence. In the present treatment, numerical solutions are obtained for a set of fluid equations derived from the moment description of a generalized gyrokinetic equation. The density, velocity, and temperature profiles in a source-driven presheath are computed, which show a dependence on the angle of incidence of the magnetic field on a perfectly absorbing solid surface.

DOI: 10.1103/PhysRevE.66.026412 PACS number(s): 52.40.Hf, 52.40.Kh, 52.30.Gz

I. INTRODUCTION

Scientific interests related to the material plasma interaction are as old as the history of laboratory plasma experiments itself. Standard notions now exist about the mechanism of plasma-wall interaction and formation of an electrostatic sheath in an unmagnetized plasma. With the increasing importance of strong magnetic fields in modern experiments, many of these standard unmagnetized results are also in use without much modifications for modeling the boundary region of strongly magnetized plasmas. An even complicated configuration, where the strong confining magnetic field is incident obliquely on the target surface, is preferred in the modern fusion experiments in order to minimize the incident heat flux. Similar configurations are also encountered, for example, on the surface of a spacecraft that receives the flux of plasma along the earth's magnetic field. A considerable interest therefore has been in analyzing the sheath and presheath structures in magnetized plasmas.

The magnetized counterparts of conventional sheath and presheath theories are widely discussed and have been central to many investigations relating to magnetized plasma-wall interaction. Most of the discussion related to the magnetized presheath and its connection to the classical Bohm sheath is based on the standard fluid model of the magnetized plasma-wall interaction. Using the standard fluid model, Chodura [1] successfully explained the results of his particle in cell simulation of a magnetized presheath, obtaining a requirement of supersonic parallel flow velocity at the entrance to a quasineutral, collisionless region called the ''magnetic presheath.'' In Chodura's simulation the magnetic presheath was seen as the region where both ions and electrons flow with equal velocity ($u_e = u_i$). Further downstream existed a narrow region where the flow velocity of electrons exceeded that of the ions ($u_e > u_i$). This imbalance results in a finite space charge as the flux, nu, of both electrons and ions remains conserved. Chodura thus concluded that there exists a double structure comprising a quasineutral magnetic presheath and a space charge dominated Debye sheath, also that a purely parallel flow in a magnetic presheath is deflected to become normal to the solid surface in order to satisfy the classical Bohm criterion [2]. A fluid approximation presented by Chodura [1] used standard fluid equations for electrons and ions to explain the numerical observations. Chodura presented a wavelike analysis to show that in a collisionless regime, the conventional fluid model yields a requirement of supersonic parallel flow, $u_\parallel \geq c_s$, at the entrance to the quasineutral magnetic presheath, where $c_s = [(T_e + \gamma T_i)/m_i]^{1/2}$, T_e is the electron temperature, T_i is the ion temperature, m_i is the ion mass, and γ is the ratio of specific heats at constant pressure and at constant volume for the ions.

The fluid model was used also by Riemann [3], who presented the theory of a collisional magnetized presheath. Riemann showed that the requirement of supersonic parallel flow could be avoided if a velocity driving mechanism (collisions or ionization) is included within the presheath region. The explicit inclusion of collisions in Riemann's analysis provides a mechanism for the flow velocity to grow from a subsonic value to the required boundary value. In the collisionless limit, Riemann also recovered the Chodura criterion using purely time independent arguments.

The Chodura and Riemann models for the magnetized presheath essentially provide connectivity to the classical Bohm criterion, thus the structure beyond the Bohm point ($u_x = c_s$, where u_x is the ion flow velocity normal to the solid surface) sees no effect of the intensity or the orientation of the magnetic field. However, there are observations where a finite departure from the conventional results could be seen. For example, in an observation on Joint European Torus (JET), Harbour and Loarte [4] reported that for the grazing incidence, the parallel Mach number at the high field side limiter plate could be substantially subsonic. They attribute this behavior of the boundary flow to either an increased magnetic field intensity or a very grazing incidence of the magnetic field to the limiter surface (see also Ref. [5]).

*Present address: Max-Planck-Institut fü Plasmaphysik, Boltzmannstr. 2, D-85748, Garching, Germany.

†Present address: 332B ESB, Electrical Engineering Dept., Indian Institute of Technology Madras, Chennai 600 036.

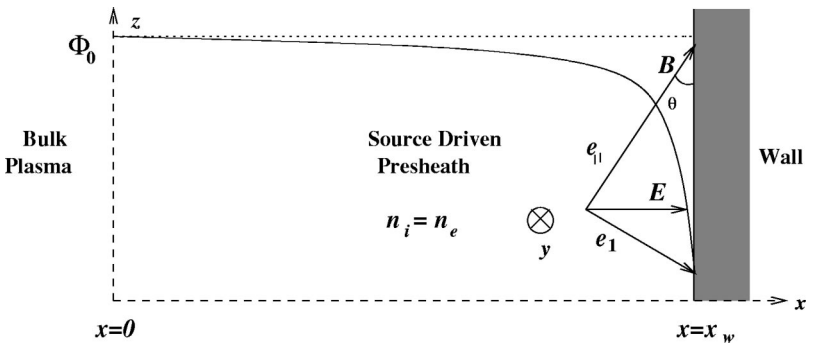

FIG. 1. Geometry of the magnetized presheath.

It is also important to notice that a nonconventional treatment of the magnetized sheath by Holland *et al.* [6] recovers no equivalent of the Bohm condition in the case of extremely grazing incidence, whereas, the conventional fluid model essentially connects to the Bohm criterion at the entrance to a magnetized sheath. These examples suggest that there are regimes where a rather careful fluid approach is required.

The departure from conventional results in strong magnetic fields indicates that the extent of magnetization of the ions plays an important role in determining the mechanism of plasma-wall interaction. Finite effects of the intensity and the obliqueness of the magnetic field thus appear on the boundary conditions at the material surface. An analysis of the intensity of collisional processes in the edge plasma for a typical fusion device [7] estimates that for the charge exchange processes a typical plasma density of 1×10^{13} cm^{-3} would yield an ion mean free path $\lambda_{cx}=25$ cm. At the same time, with a typical magnetic field of 2 T and an ion temperature of 100 eV, the mean ion Larmor radius $\rho_i\approx10^{-1}$ cm. These values give a ratio of the mean free time between ion-neutral collisions to the ion gyroperiod, $\tau_{cx}/\tau_g=2.5\times10^2$. The above analysis indicates that collisions may play only a marginal role as a velocity drivers in strongly magnetized configurations. In view of these results it becomes important to analyze the behavior of boundary conditions in a separate kind of presheath, where the velocity driver does not inject a net momentum into the system. Results of the present study show that the boundary values in a purely source-driven collisionless system do recover a finite dependence on the angle of incidence θ, as opposed to the conventional (collisional) treatment where the normal flow is generally obtained to approach a supersonic value in order to satisfy the Bohm criterion.

However, a collisionless fluid treatment is not trivial and requires some special considerations regarding the moment description of the underlying kinetic model. In the present paper we investigate a magnetized presheath driven mainly by a uniform source of plasma. An alternate set of fluid equations, as derived from the moment description of a gyrokinetic equation, is used for ions. Since large cross-field drifts are present in a magnetized oblique presheath, a generalized gyrokinetic approach as prescribed by Bernstein and Catto [8] is employed, which admits the presence of large drift velocities. Collisions are included only marginally so as not to affect the kinetic ordering of the colliding ions. In the limit of normal incidence, where the higher order drift effects vanish, it becomes possible to compare our results with the unmagnetized presheath solutions obtained by Scheuer and Emmert [9], who developed a set of fluid equations for collisional and collisionless presheath plasma assuming separate parallel and perpendicular energies. The present paper is organized as follows. In Sec. II, the standard fluid model is considered to derive and briefly discuss the Chodura criterion. The fluid equations are derived using the moment description of a gyrokinetic equation in Sec. III. The procedure for the numerical solution of fluid equations is described in Sec. IV and the results are presented and discussed in Sec. V.

II. STANDARD FLUID MODEL AND CHODURA CRITERION

The condition of supersonic ion parallel flows at the magnetized presheath edge derived originally by Chodura [1] can be obtained in a simpler way by considering the continuity and momentum equations in the conventional collisionless form

$$\nabla\cdot(n_s\mathbf{u}_s)=0, \tag{1}$$

$$m_s\mathbf{u}_s\cdot\nabla\mathbf{u}_s=q_s(\mathbf{E}+\mathbf{u}_s\times\mathbf{B})-\nabla p_s/n_s, \tag{2}$$

where q, m, n, u, and p are the charge, mass, density, flow velocity, and pressure of the species s, respectively. In this section and in the rest of the paper we follow the geometry as described in Fig. 1. The x axis is chosen to be normal to the solid surface, while the y axis points towards inside of the plane of the figure. The magnetic field **B** is incident making an angle θ with the solid surface. A field aligned set of unit vectors $(\hat{e}_\parallel,\hat{e}_1,\hat{e}_y)$ is chosen for the simplicity, such that $\hat{e}_\parallel=\hat{e}_1\times\hat{e}_y$. The components of the ion force equation (2) in the coordinates $(\hat{e}_\parallel,\hat{e}_1,\hat{e}_y)$ can now be written for a one-dimensional case by defining $u_\parallel$, u_1, u_y, and u_x as the components of $\mathbf{u}_i$ along the directions, $\hat{e}_\parallel$, $\hat{e}_1$, $\hat{e}_y$, and $\hat{e}_x$, respectively,

$$m_in_iu_xu_\parallel'=\sin\theta n_iq_iE-\sin\theta\ \ p_i', \tag{3}$$

$$m_in_iu_xu_1'=\cos\theta n_iq_iE-\cos\theta p_i'+n_iq_iu_yB, \tag{4}$$

$$m_in_iu_xu_y'=-n_iq_iu_1B, \tag{5}$$

where the prime denotes a differentiation with respect to x. Following Chodura's arguments [1] we assume the electrons to have a Boltzmann distribution [i.e., $n_e=n_0\exp(-q_e\phi/T_e)$,

where ϕ is electrostatic potential and T_e is the electron temperature] and the presheath to be quasineutral (i.e., $n_i = n_e$). Considering now the adiabatic equation of state

$$p_s' = \gamma_s T_s n_s' \tag{6}$$

allows Eq. (3) to be written as

$$m_i n u_x u_\parallel' = \sin\theta (T_e + \gamma_i T_i) n'. \tag{7}$$

At the presheath entrance, the boundary conditions consistent with an undisturbed plasma demand a purely parallel flow into the presheath. Accordingly, at the presheath edge,

$$u_{10} = u_{y0} = 0 \quad \text{and} \quad u_{x0} = u_{\parallel 0} \sin\theta. \tag{8}$$

Substituting n' from the continuity equation (1) and evaluating Eq. (7) at the presheath edge [i.e., using (8)] yields

$$(u_{\parallel 0}^2 - c_s^2) u_\parallel' = 0. \tag{9}$$

Clearly for $u_\parallel'$ to be finite at the presheath edge it is required that

$$u_{\parallel 0} = c_s, \tag{10}$$

which is the marginal form of the condition derived by Chodura and Riemann.

It is also clear from Eqs. (3) and (4) that the x component of Eq. (2) becomes

$$(u_x^2 - c_s^2) u_x' = \cos\theta \Omega_i u_y, \tag{11}$$

such that the right-hand side (rhs) of Eq. (11) resembles a velocity driver which allows the subsonic u_x in the magnetic presheath (here $\Omega_i = q_i B/m_i$). However the parallel velocity $u_\parallel$ still requires to be supersonic unless a similar term appears in Eq. (9) representing a velocity driver such as collisions or ionization. The generalization of the condition (10) allowing supersonic parallel flow at the magnetic presheath edge ($u_\parallel \geqslant c_s$) can also be understood immediately [10]. It can be readily shown that if acceleration along y ($E \times B$ inertia term) on the lhs of Eq. (5) is assumed finite at the presheath edge, Eqs. (5) and (4) suggest that u_1' is finite. In this case Eq. (9) is replaced by

$$(u_x^2 - \sin^2\theta c_s^2) = u_1' \cos\theta / u_\parallel', \tag{12}$$

i.e., the flow velocity at the magnetic presheath edge would depend upon the asymptotic behavior of ratio $u_1' \cos\theta / u_\parallel'$ as appearing on the rhs of Eq. (12). However, an asymptotic solution demanding that $u_1' \cos\theta / u_\parallel'$ should approach zero at the presheath edge would always require the parallel flow to be equal to c_s.

Since the standard fluid description (e.g., Braginskii [11]) is obtained by the procedure of Chapman and Cowling [12], i.e., by using a formal expansion of the plasma distribution function f about an equilibrium distribution in the parameter λ/L (where λ is the collision mean free path and L is the scale of variation for the macroscopic plasma parameters), the conventional fluid approach is suitable for a highly collisional regime where the collision frequency dominates the ion gyrofrequency [13]. As in the rest of this paper we aim to investigate a purely source-driven, collisionless (weakly collisional) presheath in a strongly magnetized regime, we use an alternate set of fluid equations obtained from the moment description of a generalized gyrokinetic equation [8].

III. MOMENT EQUATIONS

We adapt the moment description based formally on the generalized gyrokinetic approach of Bernstein and Catto [8]. The first application of a set of generalized gyrokinetic variables introduced by Bernstein and Catto yields $f_1 = f - f_0$, which is smaller by an order of $1/\Omega$ as compared to that in the conventional gyrokinetic theory. Thus by repeated inductions, Bernstein and Catto could evaluate f_1, which is second order in $1/\Omega$, thereby recovering a value of f_0 which is correct up to first order in $1/\Omega$. A generalization of the approach of Bernstein and Catto can be considered formally by assuming that gyrocenter variables can be found which depend on φ through order $(1/\Omega)^N$. This would then lead to a value of f_1 which is of order $(1/\Omega)^{N+1}$ and f_0 which is correct to order $(1/\Omega)^N$. The gyrokinetic prescription would be correct to all orders for $N \to \infty$.

In a one-dimensional case where variation exists only along x (see Fig. 1), we begin by considering a generalized gyrokinetic equation for the ion distribution function $f_0 = \overline{f(v_\parallel, \mu, \mathbf{r}, \varphi)}$,

$$\sin\theta \overline{v_\parallel} \frac{\partial f_0}{\partial r_x} + \cos\theta \overline{v_1} \frac{\partial f_0}{\partial r_x} + \overline{\dot{v}_\parallel} \frac{\partial f_0}{\partial v_\parallel} = c + s, \tag{13}$$

where the overline denotes a gyrophase averaging as prescribed by Bernstein and Catto [8], $\mathbf{r}, \varphi$, and μ represent the generalized gyrocenter, gyrophase, and angular momentum, respectively, while $v_\parallel$ and v_1 are the components of the generalized gyrocenter velocity along $\mathbf{B}$ and $\hat{e}_1$, respectively. The gyrocenter variables are assumed to be known to all orders to account for the large cross-field drifts [8]. The quantities c and s are the gyroaveraged contributions of collisions and source, respectively. No spatial variation is assumed along y (i.e., $\partial/\partial y = 0$), and for rest of the treatment it is understood that $\mathbf{r} \equiv x$.

As the cross-field drift $\overline{v_1}$ of an ion couples with the parallel velocity $\overline{v_\parallel} \equiv v_\parallel$ through the self-consistent presheath electric field [3] E, a nonlinear coupling $\mathcal{C}$ can now be introduced,

$$\overline{v_1} = \mathcal{C}(x, v_\parallel)\, v_\parallel. \tag{14}$$

Since in rest of the treatment we are interested in the averaged quantities, we assume the $\mathcal{C}$ to depend only on the average parallel velocity $u_\parallel = \langle v_\parallel \rangle$, where the average $\langle A \rangle$ of a function A is defined as

$$\langle A\rangle = \frac{\int A f\, d^3v}{\int f\, d^3v}. \tag{15}$$

The Eq. (14) would therefore be reduced to

$$\overline{v_1} = C(x,u_\parallel)v_\parallel = \alpha(x) \quad v_\parallel. \tag{16}$$

Coming back to Eq. (13), one can therefore rewrite it as

$$\kappa v_\parallel \frac{\partial f_0}{\partial x} + \dot{\overline{v}}_\parallel \frac{\partial f_0}{\partial v_\parallel} = c + s, \tag{17}$$

where

$$\kappa = [\sin\theta + \alpha\cos\theta] \tag{18}$$

and

$$\dot{v}_\parallel = (q_i E/m_i)\sin\theta. \tag{19}$$

The moments of gyrokinetic equation (17) produce estimations for the conservation of particles, momentum, and energy in terms of coupling $\alpha(x)$. Since the electrons are strongly magnetized and react instantaneously to potential variations along the magnetic field, their density can be given by the Boltzmann distribution. Therefore in the quasineutral region of the presheath,

$$n(x) = n_e(x) = n_0 \exp(-q_e\phi/T_e), \tag{20}$$

where ϕ is the electrostatic potential, n_0 is the density at $x=0$, and T_e is the electron temperature which is assumed constant in the region.

The source of plasma $s = s(x,v)$ is assumed to have a stationary Maxwellian velocity distribution with temperature T_s,

$$s(x,v) = s_0(x) g(v,T_s), \tag{21}$$

where the function $s_0(x)$ determines the spatial variation of the source intensity and $g(v,T)$ is a stationary Maxwellian velocity distribution with temperature T,

$$g(v,T) = (m_i/2\pi T)^{3/2} \exp(-m_i v^2/2T), \tag{22}$$

where

$$v^2 = v_\parallel^2 + v_1^2 + v_y^2. \tag{23}$$

However, we assume a uniform source and use $s_0(x) = s_0$ in the present treatment.

The weak ion-neutral collisions are modeled using a Bhatnagar-Gross-Krook (BGK)-type collision term [14]

$$c = -\nu f_0 + \nu n(x) g(v,T_n), \tag{24}$$

where ν is the ion-neutral collision frequency and $g(v,T_n)$ represents the velocity distribution of background neutrals with temperature T_n.

In general, the jth moment of the gyrokinetic equation (17) is given by

$$\kappa \frac{\partial}{\partial x}\int v_\parallel^j v_\parallel f_0 d^3v + \frac{q_i}{m_i} E_\parallel \int v_\parallel^j \frac{\partial f_0}{\partial v_\parallel} d^3v = \int v_\parallel^j (c+s) d^3v. \tag{25}$$

The values $j = 0,1$, and 2 yield particle conservation, balance of parallel momentum, and the parallel energy flux, respectively, given by the following equations:

$$\kappa \frac{\partial}{\partial x}(n u_\parallel) = s_0, \tag{26}$$

$$\kappa \frac{\partial}{\partial x}\left(n u_\parallel^2 + \frac{p_\parallel}{m_i}\right) = n\frac{q_i}{m_i} E_\parallel - \nu n u_\parallel, \tag{27}$$

$$\kappa \frac{\partial}{\partial x}\left(n u_\parallel^3 + 3 u_\parallel \frac{p_\parallel}{m_i}\right) = 2 n u_\parallel \frac{q_i}{m_i} E_\parallel + \frac{s_0}{m_i} T_s - \nu n u_\parallel^2 - \frac{\nu n}{m_i}(T_i - T_n), \tag{28}$$

where $u_\parallel$ is the flow velocity along the magnetic field and the quantities $p_\parallel$, T_s, and T_n are defined as follows:

$$p_\parallel = n T_i = \int m_i (v_\parallel - u_\parallel)^2 f_0(x,v) d^3v, \tag{29}$$

$$T_s = \int m_i v_\parallel^2 g(v,T_s) d^3v, \tag{30}$$

$$T_n = \int m_i v_\parallel^2 g(v,T_n) d^3v. \tag{31}$$

It is assumed for simplicity that the distribution remains approximately symmetric around the mean velocity, and the thermal energy flux

$$Q_t = \int m_i (v_\parallel - u_\parallel)^3 f_0(x,v) d^3v \tag{32}$$

has therefore been neglected. However, for an exact treatment a profile for Q needs to be drawn from the kinetic results [9]. Substituting Eq. (26) in Eq. (27) yields the equation of the momentum balance,

$$n u_\parallel \kappa \frac{\partial u_\parallel}{\partial x} = -\kappa \frac{\partial}{\partial x}\left(\frac{p_\parallel}{m_i}\right) + n\frac{q_i}{m_i} E_\parallel - \nu n u_\parallel - s_0 u_\parallel. \tag{33}$$

An equation of state governing the variation in ion pressure can now be derived from Eqs. (26)–(28) as follows:

$$\kappa \frac{\partial p_\parallel}{\partial x} = 3 T_i \kappa \frac{\partial n}{\partial x} + s_0 m u_\parallel + \frac{s_0}{u_\parallel}(T_s - 3T_i) + \nu m n u_\parallel - \frac{\nu n}{u_\parallel}(T_i - T_n). \tag{34}$$

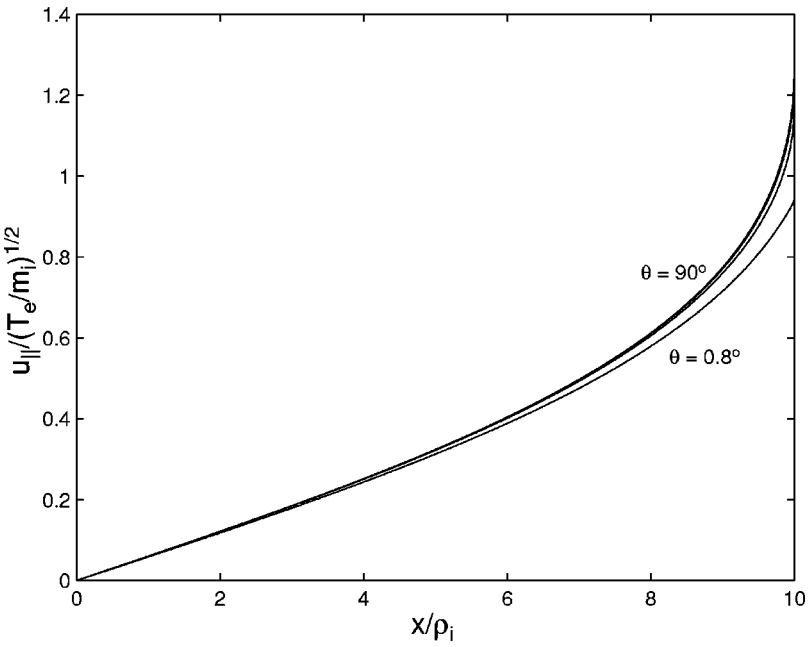

FIG. 2. Normalized parallel flow velocity $u_{\|}/(T_e/m_i)^{1/2}$; curves from bottom to top correspond to $\theta=0.8°$, 30°, 60°, and 90°.

Substituting Eq. (34) into Eq. (33) yields the equation of force balance for the ion fluid,

$$(u_{\|s}^2-u_{\|}^2)\frac{\partial u_{\|}}{\partial x}=(u_{\|s}^2+2u_{\|}^2)\frac{s_0}{\kappa n}+\frac{s_0}{\kappa n}\left(\frac{T_s-3T_i}{m_i}\right)+\frac{2\nu}{\kappa}u_{\|}^2-\frac{\nu}{\kappa}\left(\frac{T_i-T_n}{m_i}\right), \tag{35}$$

where the quantity $u_{\|s}$ is similar to a local sound velocity

$$u_{\|s}^2=\frac{1}{\kappa}\left[\sin\theta\left(\frac{T_e+3T_i}{m_i}\right)+\alpha\cos\theta\left(\frac{3T_i}{m_i}\right)\right]. \tag{36}$$

The second term in relation (36) represents the additional contribution arising from the random component of the drift generated due to the coupling of the drift $\overline{v_1}$ with the random parallel velocity $(v_{\|}-u_{\|})$. We now write the particle conservation equation (26) in the form

$$\kappa\frac{\partial n}{\partial x}=\frac{1}{u_{\|}}\left(s_0-n\kappa\frac{\partial u_{\|}}{\partial x}\right). \tag{37}$$

Each of the coupled equations (37), (35), and (34) has a singularity at $u_{\|}=u_{\|s}$ through the derivative $\mathrm{d}u_{\|}/\mathrm{d}x$. The velocity at the singular point differs from the usual ion acoustic speed c_s as a consequence of coupling between parallel and perpendicular velocities given by Eq. (16). Besides this, the singularity at $u_{\|}=0$ in Eq. (34) indicates that at the singular point $x=0$, the value of the parallel ion temperature T_{i0} is determined by the source and neutral temperatures, T_s and T_n, respectively. However, the relationship between the parameters at $x=0$ would depend upon the values of derivatives of the density and temperature. A suitable option is to assume $x=0$ as a point of symmetry such that both these derivatives could be set to zero and T_{i0} could be determined for given values of T_s and T_n. The starting value T_{i0} of the ion temperature is therefore obtained by substituting

$$\frac{\partial n}{\partial x}=0,\quad \frac{\partial p_{\|}}{\partial x}=0,\quad \text{and}\quad u_{\|}=0 \tag{38}$$

in Eqs. (37) and (34), which yields

$$n_0=s_0\left(\kappa\frac{\partial u_{\|}}{\partial x}\bigg|_{x=0}\right)^{-1} \tag{39}$$

$$\text{and}\quad T_{i0}=\frac{s_0T_s+\nu n_0T_n}{3s_0+\nu n_0}. \tag{40}$$

It is clear from Eq. (39) that s_0 scales with the bulk density $n(x=0)=n_0$. As no collisional coupling is assumed between parallel and perpendicular temperatures, the latter remains unchanged in the presheath and is equal to the source temperature T_s. Since the ion Larmor radius ρ_i is determined by perpendicular temperature $T_{\perp}$, T_{i0} relates to ρ_i through Eq. (40).

IV. NUMERICAL SOLUTIONS OF THE FLUID MODEL

As the present treatment assumes that the cross-field drifts of ions are known to all orders and the coupling $\alpha=u_1/u_{\|}$ can be derived exactly for the ions, obtaining the solutions of fluid equations (34), (35), and (37) requires u_1 and $u_{\|}$ be determined self-consistently. In a collisionless (or weakly collisional) steady state, the transverse flow velocities u_1 and u_y are the averages $\langle\overline{v_1}\rangle$ and $\langle\overline{v_y}\rangle$, which evolve according to the transverse equations

$$u_x\frac{\partial u_1}{\partial x}=\frac{q_i}{m_i}E\cos\theta+\frac{q_i}{m_i}u_yB, \tag{41}$$

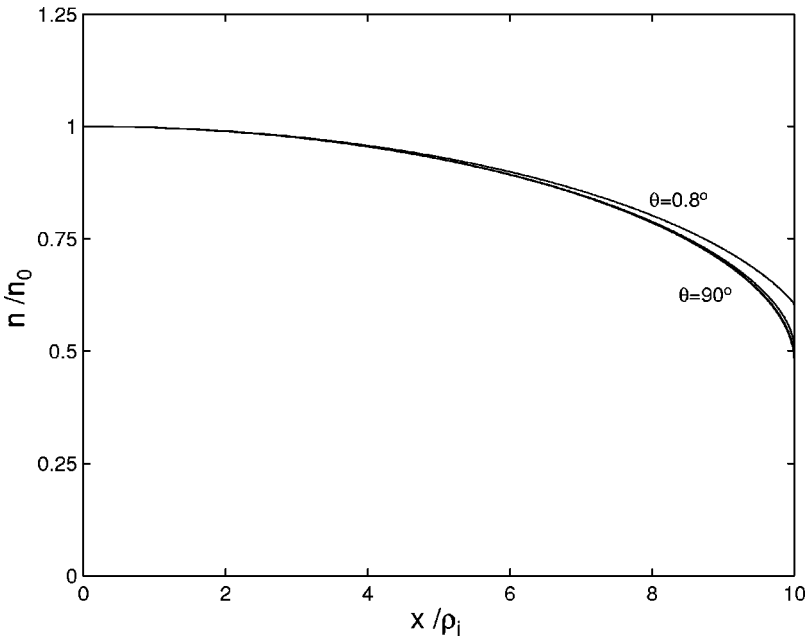

FIG. 3. Normalized density n/n_0; curves from top to bottom correspond to $\theta=0.8°$, 30°, 60°, and 90°.

$$\text{and} \quad u_x \frac{\partial u_y}{\partial x} = -\frac{q_i}{m_i} u_1 B, \tag{42}$$

when they are solved with the asymptotic starting values obtained from the approximation of "weak inhomogeneity" [3]. Here $u_x=(\sin\theta u_\parallel+\cos\theta u_1)$. Equations (41) and (42) are therefore integrated numerically along with the fluid equations (34), (35), and (37) to calculate α self-consistently. In order to determine the suitable boundary conditions for nonoscillatory solutions, Eqs. (41) and (42) are considered at the bulk presheath interface, where the gradients of the cross-field velocities vanish providing the starting values

$$u_1=0 \quad \text{and} \quad u_y=(E/B)\cos\theta. \tag{43}$$

The starting value of parallel velocity gradient, $\Delta u_\parallel/\Delta x$, is determined from the desired value of density at $x=0$, in accordance with Eq. (39). It is also important that the integration could be started only from the location $x=\Delta x$ and not from $x=0$, thereby avoiding the occurrence of a logarithmic divergence of the density [15] at $x=0$, where $E \to 0$. The equations are thus integrated until the singularity $u_\parallel=u_{\parallel s}$ is encountered.

V. RESULTS AND DISCUSSION

We now discuss the numerical solutions for the collisionless case with $\nu=0$. The results presented here all correspond to the choice $T_s=T_e$ and the presheath region which measures $10\rho_i$ along x. The parallel velocity $u_\parallel$ as a function of x/ρ_i is plotted at various values of θ in Fig. 2, which shows that at normal incidence ($\theta=90°$), the singularity $u_\parallel=u_{\parallel s}$ occurs at its conventional value of the local sound velocity $c_s=[(T_e+\gamma T_i)/m_i]^{1/2}$ (though lower than the value c_{s0} as the ion temperature drops below T_{i0} with x). However, at oblique incidences ($\theta<90°$) an additional effect is present due to the presence of nonzero cross-field flows, and the singularity occurs at $u_\parallel=u_{\parallel s}<c_s$, i.e., at a value smaller than the local sound velocity c_s, where the relation between $u_{\parallel s}$ and c_s is described by Eq. (36). Thus at the oblique incidence an additional drop is present in the parallel velocity at the sheath edge. The profile of $u_\parallel$ (and the other moments) for $\theta=60°$ remains indistinguishable from that for 90° due to a very small variation at the larger angles.

The density profiles are plotted in Fig. 3. There is an expected density drop across the presheath of approximately $n_0/2$ at the normal incidence ($\theta=90°$). As opposed to the isothermal treatments [16–19], the density does not drop ex-

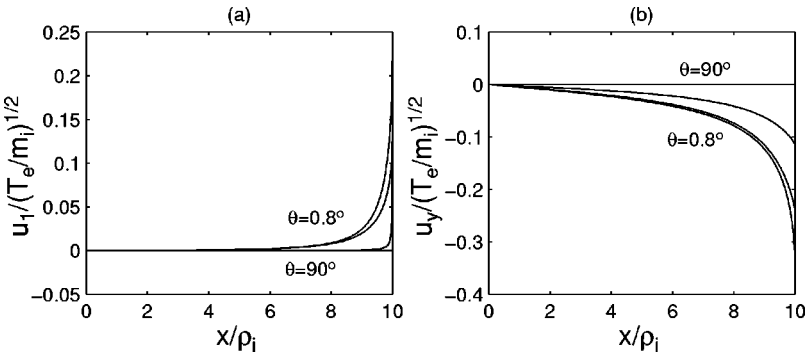

FIG. 4. Normalized transverse flow velocities; curves representing (a) $u_1/(T_e/m_i)^{1/2}$ (from top to bottom) and (b) $u_y/(T_e/m_i)^{1/2}$ (from bottom to top) correspond to $\theta=0.8°$, 30°, 60°, and 90°.

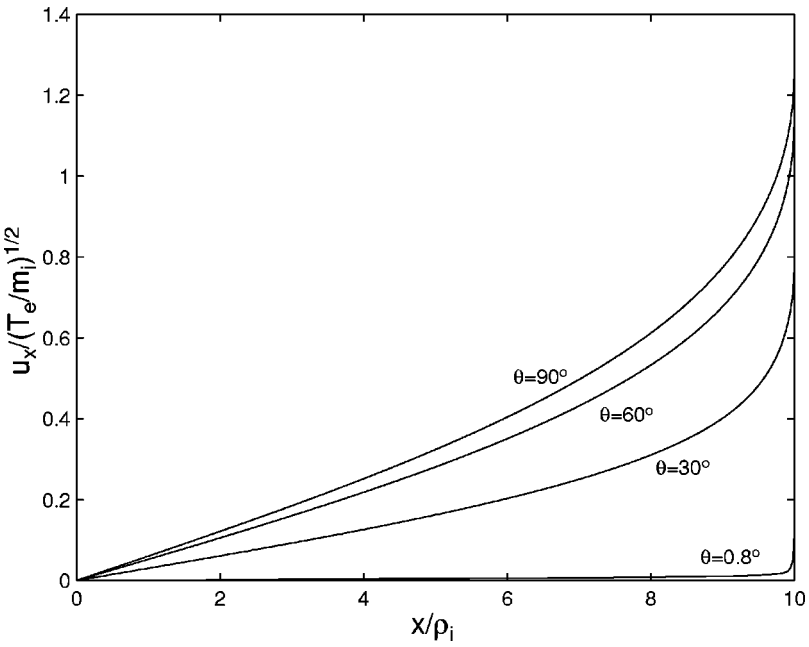

FIG. 5. The normal flow velocity u_x normalized to $(T_e/m_i)^{1/2}$; curves from bottom to top correspond to $\theta=0.8°$, 30°, 60°, and 90°.

actly to half of its bulk value n_0, since ion temperature is allowed to vary according to the equation of state (34). A smaller density drop is recovered with the angle θ becoming smaller.

Cross-field flows u_1 and u_y are plotted in Fig. 4 for various values of θ. Both the transverse flows are zero in the case of normal incidence ($\theta=90°$). The flow u_1 shows a maxima at an intermediate angle and reduces sharply as $\theta \rightarrow 0$. This confirms that u_1 is similar to an averaged polarization drift effect (proportional to the product of E_1' and $u_{\|}\sin\theta$), which is nonzero only at the oblique incidence [20] ($0°<\theta<90°$).

Interestingly, the magnitude of u_1 becomes sufficiently high and almost comparable to u_y at certain angles. This also indicates that at small to intermediate angles u_1 makes a significant contribution to the normal flow u_x. A strong dependence of angle θ can be seen on the value of normal flow u_x as plotted in Fig. 5, where u_x tends to vanish at smaller θ. A difference is evident from the conventional fluid solutions where profiles for u_x with different θ converge to a unique value c_s at the sheath edge. The parallel ion temperature T_i as plotted in Fig. 6 shows a drop at all values of angle θ. However the drop reduces with angle θ becoming smaller, showing that the maximum cooling occurs at the normal incidence. This observation, in view of a reducing $u_{\|}$ at the sheath edge, confirms that the parallel velocity indeed becomes subsonic at the sheath edge with reducing θ. Also the value of T_i at $x=0$ is $T_s/3$ in accordance with Eq. (40).

The case $\theta=90°$ could be compared with a collisionless unmagnetized case as studied by Scheuer and Emmert [9].

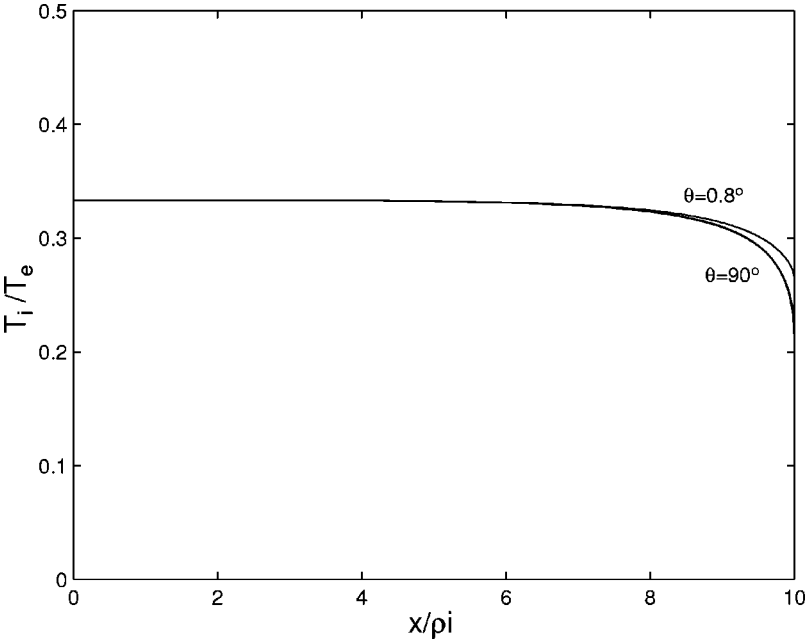

FIG. 6. Normalized parallel temperature T_i/T_e; curves from bottom to top correspond to $\theta=0.8°$, 30°, 60°, and 90°.

TABLE I. Values of density, parallel velocity, and parallel temperature at the wall, obtained in the present treatment as $\theta \to 90°$, and those reported by Scheuer and Emmert for a collisionless unmagnetized case.

	Present treatment			Scheuer and Emmert
Moments	$\theta = 70°$	$\theta = 80°$	$\theta = 90°$	Unmagnetized
n [a]	0.497	0.496	0.495	0.486
$u_\parallel$ [b]	1.204	1.209	1.212	1.220
T_i [c]	0.225	0.225	0.225	0.162

[a]Normalized to n_0.
[b]Normalized to $(T_e/m_i)^{1/2}$.
[c]Normalized to T_e.

Since no transverse flow exists, in this case the values of n, $u_\parallel$, and T_i at the solid surface show a reasonable agreement with the collisionless results of Scheuer and Emmert as presented in Table I.

For the minimum value of the angle of incidence for which numerical solutions are obtained ($\theta = 0.8°$), the flow $u_\parallel$ approaches the singularity at a considerably smaller value compared to local c_s. This limitation of the model could be explained in the following terms. As can be seen from Fig. 5, the normal velocity u_x, which is equal to the parallel velocity $u_\parallel$ for $\theta = 90°$, becomes very small as $\theta \to 0$. This happens as only a small u_1 could be generated and also the flow $u_\parallel$ in this case has a very small x component. No transport to the wall therefore is possible in the present model in extremely grazing incidences. In order to recover a sufficient u_x in an extremely grazing or wall parallel magnetic field, either an $E \times B$ friction [3] or some other external mechanism (e.g., a turbulent electric field [6] E_y) must be present. This could be verified by introducing a frictional term $-\nu_y f$ in Eq. (42), and the resulting profiles for u_x are presented in Fig. 7, where a friction is allowed ($\nu_y \neq 0$) along y. The normal flow velocity u_x plotted for different values of ratio $\delta = \nu_y/\Omega_i$ shows that a finite ν_y does enhance the magnitude of u_x even when the angle θ approaches zero. To lowest order, a collisional diffusion in the present gyrokinetics based model is the result of an effective $F \times B$ drift in the gyrokinetic equation, where F represents an average change in the translational momentum of an ion gyrocenter over a single gyroperiod due to the collisions. The collision frequency ν as included in Eq. (35) therefore does not produce any zero-order drift along $\hat{e}_1$. However, the temperature T_i in the $\nu \neq 0$ case would depend upon the absolute value of source strength s_0. This is evident from the relation (40), since if ν is finite, the value T_{i0} at $x = 0$ depends upon the factor s_0/n_0, whereas T_{i0} is independent of s_0 or n_0 and is equal to $T_s/3$ in the collisionless presheath ($\nu = 0$).

To summarize, in this paper we have analyzed the structure of a source-driven magnetized presheath when the magnetic field is at an angle to the solid surface. In contrast to a collisional presheath, the boundary value of normal flow does show a strong dependence on the angle of incidence θ in a source-driven presheath. In the cases of oblique incidence the parallel and normal flow velocities approach subsonic values at the sheath edge, while, at very grazing incidence a flow to the solid surface is possible only by means of an alternate mechanism, e.g., friction along the $E \times B$ direction or an external electric field along y.

It should, however, be emphasized that the kinetic effects (e.g., open and closed orbit structures [21] and a preferential loss of ions [6]) become important very close to the solid surface, as no mechanism is present to isotropize the velocity distribution of ions in a collisionless case [13]. A purely kinetic treatment of a source-driven oblique presheath which also connects asymptotically to a quiescent bulk is therefore nontrivial, and a careful numerical approach [22] is necessary. Finally, the sheath singularity persisting in current solutions suggests that an electrostatic sheath must be present, whose function is to ensure an equal amount of flux of electrons to the absorbing surface, the standard Bohm sheath

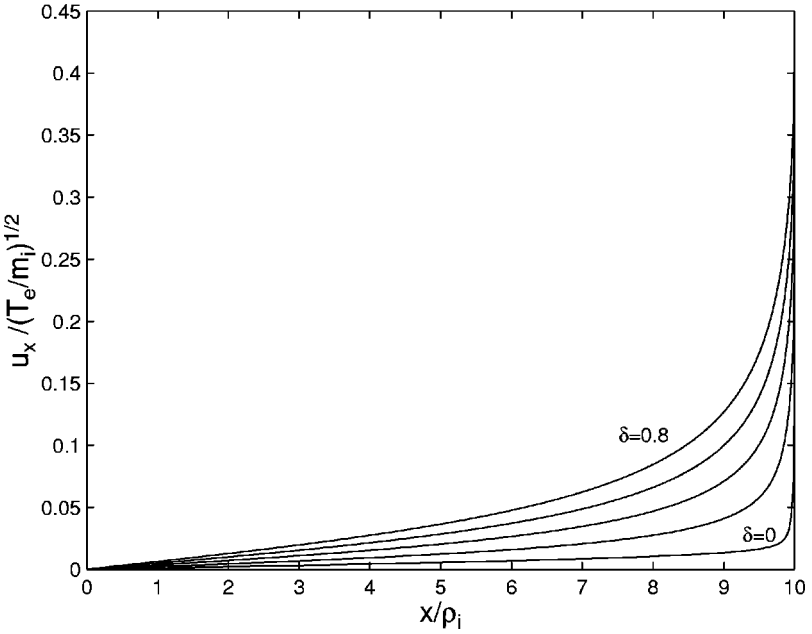

FIG. 7. The normal flow u_x normalized to $(T_e/m_i)^{1/2}$; curves from top to bottom correspond to $\delta = \nu_y/\Omega_i = 0$, 0.2, 0.4, 0.6, and 0.8.

model however accepts only a supersonic entrance velocity. The possibility of an alternate mechanism should therefore be discussed, which replaces the conventional Bohm sheath in the magnetized regime. It is worthwhile here to mention that the nonconventional treatment of the magnetized sheath by Holland *et al.* [6], which uses the kinetic ion-loss effects, could provide an alternate mechanism for ensuring an equal flux of electrons and ions to the absorbing surface while eliminating the requirement of the Bohm criterion at very grazing incidence to the solid surface. However, a smooth transition to such a magnetized sheath would essentially involve reconsidering the present gyrokinetics based presheath model with an enhanced cross-field mobility of ions (comparable to the electron mobility along the field lines) arising mainly from the kinetic ion-loss effects at grazing incidence.

ACKNOWLEDGMENT

D.S. would like to thank Dr. R. Ganesh for the helpful discussions.

[1] R. Chodura, Phys. Fluids **25**, 1628 (1982).
[2] D. Bohm, in *The Characteristics of Electrical Discharges in Magnetic Fields*, edited by A. Guthrie and R. K. Wakerling (McGraw-Hill, New York, 1949), Chap. 3, pp. 77–86.
[3] K.U. Riemann, Phys. Plasmas **1**, 552 (1994).
[4] P.J. Harbour and A. Loarte, Nucl. Fusion **35**, 759 (1995).
[5] P.C. Stangeby, C.S. Pitcher, and J.D. Elder, Nucl. Fusion **32**, 2079 (1992), and references therein.
[6] D.L. Holland, B.D. Fried, and G.J. Morales, Phys. Fluids B **5**, 1723 (1993).
[7] T.Q. Hua and J.N. Brooks, Phys. Plasmas **1**, 3607 (1994).
[8] I.B. Bernstein and P.J. Catto, Phys. Fluids **28**, 1342 (1985).
[9] J.T. Scheuer and G.A. Emmert, Phys. Fluids B **2**, 445 (1990).
[10] P.C. Stangeby, Phys. Plasmas **2**, 702 (1995).
[11] S.I. Braginskii, Rev. Plasma Phys. **1**, 205 (1965).
[12] S. Chapman and T. G. Cowling, *Mathematical Theory of Non-uniform Gases* (Cambridge University Press, Cambridge, England, 1953).
[13] E. Zawaideh, N.S. Kim, and F. Najmabadi, Phys. Fluids B **2**, 647 (1990).
[14] P.L. Bhatnagar, E.P. Gross, and M. Krook, Phys. Rev. **94**, 511 (1954).
[15] R.H. Cohen and D. Ryutov, Comments Plasma Phys. Controlled Fusion **16**, 255 (1995).
[16] L.C. Woods, J. Fluid Mech. **23**, 315 (1965).
[17] S.A. Self and H.N. Ewald, Phys. Fluids **9**, 2486 (1966).
[18] G.S. Kino and W.K. Shaw, Phys. Fluids **9**, 587 (1966).
[19] P.C. Stangeby and G.M. McCracken, Nucl. Fusion **30**, 1225 (1990).
[20] D. Sharma and H. Ramachandran, J. Plasma Fusion Res. **3**, 218 (2000).
[21] R.H. Cohen and D.D. Ryutov, Phys. Plasmas **5**, 808 (1998).
[22] D. Sharma and H. Ramachandran, J. Nucl. Mater. **290-293**, 725 (2001).